AN ABSTRACT OF THE THESIS OF

Robert Lloyd Smith for the Doctor of Philosophy in Oceanography
(Name) (Degree) (Major)

Date thesis is presented 13 May 1964

Title AN INVESTIGATION OF UPWELLING ALONG THE OREGON COAST

Abstract approved Redacted for Privacy
(Major Professor)

The oceanic phenomenon of upwelling along the Oregon coast is examined. Upwelling in both the open ocean and coastal regions is discussed. An idealized model is used, envisaging the ocean off Oregon to consist of homogeneous surface and deep layers separated by a pycnocline. The equations of motion are solved to yield the vertical velocity at the base of the surface layer. A comparison is made between the model and results inferred from hydrographic data.

In the open ocean region qualitative agreement is observed between the wind stress curl and the depth of the surface layer. Geostrophic meridional transports relative to the 1000 decibar surface were computed and found to be of the order of the uncertainty. In the coastal upwelling region surface layer zonal transports were computed from the meridional component of the mean wind stress and compared with values inferred from oceanographic data. Coastal upwelling along the Oregon coast is clearly associated with the northerly (longshore) component of the wind stress.

AN INVESTIGATION OF UPWELLING ALONG THE OREGON COAST

by

Robert Lloyd Smith

A THESIS

submitted to

OREGON STATE UNIVERSITY

in partial fulfillment of
the requirements for the
degree of

DOCTOR OF PHILOSOPHY

June 1964

APPROVED:

Redacted for Privacy

Professor of Oceanography

In Charge of Major

Redacted for Privacy

Chairman, Department of Oceanography

Redacted for Privacy

Dean of Graduate School

Date thesis is presented 13 May 1964

Typed by Rose Bethel

AN INVESTIGATION OF UPWELLING ALONG THE OREGON COAST

by

Robert Lloyd Smith

TABLE OF CONTENTS

FIGURES

TABLES

AN INVESTIGATION OF UPWELLING ALONG THE OREGON COAST

I INTRODUCTION

Along the coast of Oregon, and characteristically off the western coasts of the continents in the middle latitudes, there occurs a strip of cold coastal water. This coastal water is considerably lower in temperature than the surface waters further from the coast at the same latitude. The band of cold coastal water may appear seasonally, as off the west coast of North America, or it may be a semi-permanent feature as off south-west Africa. The difference between the water temperature at ten meters depth measured at five nautical miles, and at 85 to 165 nautical miles, off Newport, Oregon is shown in Figure 1. This is called the temperature anomaly at five miles.

The eastern boundary currents that flow along the western coasts of the continents flow equatorward from relatively high latitudes. It is therefore to be expected that the waters along the eastern edge of the ocean will be at lower temperatures than those of comparable latitude in the central regions of the ocean. For some time it was thought that the cold coastal water was simply water advected from higher latitudes by the currents. As the charts of the sea surface temperature became more complete it was evident that the temperature of the

water along the coast did not increase monotonically with decreasing latitude. Indeed, the coldest coastal water might be found far downstream. The distribution of other properties, e. g. salinity, oxygen concentration and phosphate, suggested that vertical motions were involved.

De Tessan as early as 1844 explained the cool water off Peru as the result of upwelling, according to Gunther (11, p. 112). This view was not widely accepted until early in this century when the first satisfactory physical explanation for upwelling was given. The work of Ekman (5) in 1905 provided the basis for our present day understanding of the effect of wind stress on the sea surface. Ekman showed that due to the effect of the earth's rotation and frictional forces, the net transport of water due to the wind stress is directed 90 degrees to the right (left) of the wind in the Northern Hemisphere (Southern Hemisphere). It was thus seen that a wind blowing parallel to the coast could transport water offshore and necessitate a compensatory replenishment of water from deeper layers. The theory of Ekman and the theories of upwelling evolving from it are discussed in more detail in Section II.

Because the upwelling process brings subsurface water into the surface layer, it induces horizontal anomalies in the distribution of physical and chemical properties that normally have marked vertical

gradients. Such anomalies are sometimes used as indicators of upwelling (25). Upwelling has important effects, particularly on the marine biological environment. Upwelling is of great importance to the productivity of coastal water because it brings nutrients, whose concentrations normally increase with depth, into the euphotic zone. The incredibly rich population of marine life off the coast of Peru, and the guano industry there, are due to the effects of upwelling enriching the surface water. Upwelling also has marked effects on local climate. Cool air temperatures and coastal fog are frequently associated with upwelling.

A Definition of Upwelling

Wyrtki (51, p. 314) has pointed out that although upwelling is a term widely used in oceanography a precise definition has not yet been given. Vertical motion is an integral part of oceanic circulation, but ascending motions in any depth are not considered upwelling unless they reach the surface layer. A maximum of vertical motion that Stommel (35) shows is associated with the depth of no meridional geostrophic flow cannot be considered upwelling since it is restricted to relatively great depths. Sverdrup (38, p. 318) states upwelling implies that subsurface water is continually or intermittently drawn to the surface and spread outward from the area of upwelling.

Upwelling will be defined here as an ascending motion of some minimum duration and extent by which water from subsurface layers is brought into the surface layer and is removed from the area of upwelling by horizontal flow. The water usually comes from depths not exceeding 200 meters (39, p. 501).

There must be a distinction between the effects of upwelling and the physical process of upwelling itself. It is usually true that the physical and chemical properties in the region of upwelling are altered and show anomalies, if these properties have a vertical gradient. But it is also true that effects similar to those produced by upwelling can be caused by wind induced vertical mixing or by a baroclinic adjustment of the mass field associated with an increase in the geostrophic transport of the coastal current.

Regions of Upwelling

It is along the western coasts of the continents that the eastern boundary currents flow, and it is there also that the relative orientation of the predominant wind to the coastline is suitable for sustained upwelling. Many of the descriptive studies of upwelling are included in the more extensive studies of the major eastern boundary currents. It will be convenient for this reason to refer to some of the major upwelling regions by the name of the current in the region. Mention

will be made of the more important descriptive studies of upwelling. The theoretical and the more quantitative studies will be discussed in Section II.

The California Current. Along the coasts of Washington, Oregon, California and Baja California, upwelling is a seasonal feature. Its occurrence coincides with the strongest northerly winds, which occur off Baja California and southern California in the spring and off the northern coasts in the summer. Upwelling occurs off Washington in the late summer (27) but not with the intensity observed off Oregon. A recent discussion of upwelling along the west coast of North America is given in the work of Reid, et al. (30) on the California Current system.

The Peru Current. Usually a southerly wind blows parallel to the Peruvian Coast causing the transport of surface waters away from the coast and subsequent upwelling between about five degrees and 20 degrees south latitude. Sufficient oceanographic observations are not yet available to define the seasonal variations. Wooster (46) has studied the surface temperatures and finds upwelling most intense during the southern winter and absent or least intense in the summer. The catastrophic oceanic disturbance, El Nino (the Child), is so named since it usually occurs after Christmas. El Nino can be defined as

the set of conditions causing extended weakening or cessation of upwelling. The reduction of the nutrient supply and the warmer water drives away the familiar marine life. Gunther (11, p. 196-218) studied the region in 1936 and found evidence of upwelling as far south as 35 degrees. He studied the distribution of salinity and temperature and made estimates of the depth from which the upwelled water came. The estimates varied from 87 to 177 meters. More recently Posner (28) studied the Peru Current and gave estimates of the volume of water taking part in the upwelling process and the amounts of nutrients involved. Wyrtki (51) has investigated quantitatively the relation between coastal upwelling and the horizontal circulation in the Peru Current.

The Benguela Current. The Benguela Current is a major oceanographic feature of the southwest coast of Africa. The region from the neighborhood of Cape Town to about 15 degrees south latitude is an area of upwelling and cold, fertile water. Upwelling appears to be a permanent feature, reaching a maximum in the southern summer. The upwelling in the region has been studied recently by Currie (3) and Hart and Currie (13, p. 184-192).

The Canary Current. Off the north west coast of Africa, from 15 to 30 degrees north latitude, there appears to be a semipermanent

region of upwelling (47, p. 272), which has not been studied very thoroughly.

Australia. It was anticipated that upwelling would exist in the Indian Ocean along the northwest Australian coast. Wyrtki (50) found that the atmospheric circulation is apparently unfavorable and while upwelling may occasionally occur it is not strong. The major area of upwelling is between Java and Australia during the southeast monsoon season (May to September). The most intense upwelling occurs along the south coast of Java and Sumbawa. The relation between wind stress and upwelling is qualitatively confirmed in the region.

Other Regions. While the major areas of upwelling are along the western coasts, upwelling is not a phenomenon unique to eastern boundary currents. It has been observed in the eastern end of the Gulf of Cariaco on the Caribbean coast of Venezuela (31, p. 170). Upwelling of a more limited extent has been observed off the northeastern coast of Florida (10, 40) and North Carolina (44). A correlation with the wind has been observed in upwelling off Nova Scotia (12, 16). Upwelling also occurs in such relatively small bodies of water as Lake Michigan (22).

In summary: Upwelling appears to occur where the winds are

favorable to transport water offshore. The major atmospheric circulation is favorable to upwelling over extended regions and periods on the western coasts of the continents. It is here that the major areas of upwelling are found.

II. REVIEW OF THEORETICAL STUDIES OF UPWELLING

The Basic Equations

The equations of motion are referred to a right handed Cartesian coordinate system rotating with the earth. The positive x-axis is directed eastward, the y-axis northward, and the z-axis upward, with the origin at the mean free surface of the ocean. The equations of motion in the form usual for oceanographic applications are (36, p. 649):

$$\frac{du}{dt} = -\frac{1}{\rho}\frac{\partial p}{\partial x} + fv + \frac{1}{\rho}A_H\left(\frac{\partial^2 u}{\partial x^2} + \frac{\partial^2 u}{\partial y^2}\right) + \frac{1}{\rho}\frac{\partial}{\partial z}\left(A_V\frac{\partial u}{\partial z}\right) \qquad (1)$$

$$\frac{dv}{dt} = -\frac{1}{\rho}\frac{\partial p}{\partial y} - fu + \frac{1}{\rho}A_H\left(\frac{\partial^2 v}{\partial x^2} + \frac{\partial^2 v}{\partial y^2}\right) + \frac{1}{\rho}\frac{\partial}{\partial z}\left(A_V\frac{\partial v}{\partial z}\right) \qquad (2)$$

$$\frac{dw}{dt} = 0 = -\frac{1}{\rho}\frac{\partial p}{\partial z} - g \qquad (3)$$

A complete list of symbols is given in the appendix. The Reynolds stresses have been expressed in terms of eddy viscosities and velocity gradients (39, p. 475). The horizontal eddy viscosity is assumed constant. The horizontal component of the Coriolis force, $-2\omega w \cos\varphi$, has been neglected in equation (1) and the vertical component, $2\omega u \cos\varphi$, in equation (3). Since the vertical accelerations and the

frictional forces have been neglected in equation (3), this is the hydrostatic relation. To these equations is added the equation of continuity:

$$\frac{\partial u}{\partial x} + \frac{\partial v}{\partial y} + \frac{\partial w}{\partial z} = -\frac{1}{\rho}\frac{d\rho}{dt} \tag{4}$$

Further simplifications are usually introduced in the above equations, depending on the character of the problem. In particular, the nonlinear inertial acceleration terms are often neglected in the equations of motion. Sea water may be considered incompressible, reducing the equation of continuity to

$$\frac{\partial u}{\partial x} + \frac{\partial v}{\partial y} + \frac{\partial w}{\partial z} = 0 \tag{5}$$

These simplifications will be found in the theories discussed.

The Theory of Ekman

Ekman (5) in his classic paper of 1905, "On the influence of the earth's rotation on ocean-currents," was the first to give mathematical form to the effects of the Coriolis force and friction on ocean currents. This work provided the basis for the physical explanation of upwelling as well as the effects of wind stress on the sea.

Ekman assumed a steady state of motion in a uniform and homogeneous ocean of infinite extent, with a steady and uniform wind blowing on the surface. The equations of motion are then:

$$0 = fv + \frac{1}{\rho}\frac{\partial}{\partial z}\left(A_V \frac{\partial u}{\partial z}\right)$$

$$0 = -fu + \frac{1}{\rho}\frac{\partial}{\partial z}\left(A_V \frac{\partial v}{\partial z}\right) \qquad (6)$$

As boundary conditions, it is assumed that the velocities and velocity gradients vanish in the ocean depths and that at the sea surface the wind stress equals the shearing stress in the fluid:

$$\tau_x = A_V \frac{\partial u}{\partial z}\bigg|_{z=0} \qquad \text{and} \qquad \tau_y = A_V \frac{\partial v}{\partial z}\bigg|_{z=0} \qquad (7)$$

Under these boundary conditions the integral form of the equations gives the mass transport caused by the wind:

$$M_x = \int_{-\infty}^{0} \rho u \, dz = \frac{\tau_y}{f}$$

$$M_y = \int_{-\infty}^{0} \rho v \, dz = -\frac{\tau_x}{f} \qquad (8)$$

These components of the wind induced mass transport are commonly referred to as the Ekman transports. The relation between the Ekman transport and the wind stress is independent of the manner of dependence of and A_V on depth.

Under the more restrictive assumption of an eddy viscosity constant with depth, Ekman showed that the velocity decreased

exponentially with depth. The velocity is reduced to $1/e^{\pi}$ of its surface value at a depth

$$Z = D_V = -\pi\sqrt{\frac{A_V}{\rho\omega\sin\varphi}} \tag{9}$$

This depth, D_v, called the depth of frictional influence or the depth of the wind current, is generally of the order of 100 meters (5, p. 12). The wind stress thus exerts an influence on only a relatively thin layer of the ocean. Equations (8) would be valid to a good approximation with the lower limits being the depth of frictional influence. Thus the Ekman transport is confined to approximately the upper 100 meters.

The result of Ekman, that the net transport of water due to the wind is directed at right angles to the wind stress, provided the first satisfactory explanation of the process of upwelling. At least a qualitative agreement between the occurrence of upwelling and the component of the wind parallel to the coast should be expected. In the Northern Hemisphere, the component of the wind stress parallel to the coast and directed from right to left looking offshore would transport water offshore and necessitate the rise of deeper water near the coast. The component of the mean wind stress parallel to the Oregon coast is shown in Figure 1 along with the observed temperature anomaly.

McEwen in 1912 (19) applied the theory of Ekman to the west coast of North America. He showed that the temperature anomalies observed were in satisfactory agreement with those predicted on the basis of the theory. Values of the horizontal transport of upwelled water off the coast of southern California were calculated by Sverdrup and Fleming in 1941 (38, p. 319-328). Vertical displacements of temperature, salinity, and oxygen concentration were studied to determine the vertical velocities. The offshore transport of water computed from continuity considerations agreed well with the transport predicted by equations (8).

Welander generalized the theory of Ekman in 1957 (43) to include a shallow sea where the depth, b, is less than the depth of frictional influence. Retaining the assumption of homogeneous water and steady state but including the horizontal pressure gradients due to slope of the sea surface, the equations are:

$$0 = -g\frac{\partial \xi}{\partial x} + fv + \frac{A_v}{\rho}\frac{\partial^2 u}{\partial z^2}$$

$$0 = -g\frac{\partial \xi}{\partial y} - fu + \frac{A_v}{\rho}\frac{\partial^2 v}{\partial z^2} \qquad (10)$$

With the same surface boundary conditions as before but with the lower boundary condition being that the velocity vanishes at the bottom,

Welander obtains the following for net mass transport:

$$M_x = C\frac{\tau_x}{f} - D\frac{\tau_y}{f} + \frac{\rho g b}{f}\left(E\frac{\partial \xi}{\partial x} - F\frac{\partial \xi}{\partial y}\right)$$

$$M_y = D\frac{\tau_x}{f} + C\frac{\tau_y}{f} + \frac{\rho g b}{f}\left(F\frac{\partial \xi}{\partial x} + E\frac{\partial \xi}{\partial y}\right) \qquad (11)$$

The expressions for C, D, E and F are involved functions of the ratio of depth to the depth of frictional influence, but for this ratio greater than one yield:

$$M_x = \frac{\tau_y}{f} - \frac{\rho g b}{f}\frac{\partial \xi}{\partial y}$$

$$M_y = -\frac{\tau_x}{f} + \frac{\rho g b}{f}\frac{\partial \xi}{\partial x} \qquad (12)$$

The total mass transport is thus the sum of the Ekman transport (the wind induced transport) and the geostrophic transport. For the depth less than one-half of the depth of frictional influence, the variation of C, D, E and F shifts the direction of the Ekman transport toward the direction of the wind. It is thus possible for upwelling to be induced in a very shallow sea or lake by an offshore wind. The continental shelf along the Oregon coast is sufficiently deep to ignore the effect of the ocean depth on the Ekman transport.

The Theory of Hidaka

A steady state theory of upwelling in a homogeneous ocean was developed by Hidaka in 1954 (14). The wind is confined to a belt of width L along a straight coast. The coastline is defined by the line x=0. Assuming no variations in the longshore direction, the horizontal equations of motion and the equation of continuity are written

$$0 = -g\frac{\partial \xi}{\partial x} + fv + \frac{A_H}{\rho}\frac{\partial^2 u}{\partial x^2} + \frac{A_V}{\rho}\frac{\partial^2 u}{\partial z^2}$$

$$0 = -fu + \frac{A_H}{\rho}\frac{\partial^2 v}{\partial x^2} + \frac{A_V}{\rho}\frac{\partial^2 v}{\partial z^2} \tag{13}$$

$$\frac{\partial u}{\partial x} + \frac{\partial w}{\partial z} = 0 \tag{14}$$

The boundary conditions are:

$$A_V \frac{\partial u}{\partial z}\bigg|_{z=0} = 0 \qquad \text{for} \quad 0 \leq x < \infty$$

$$A_V \frac{\partial v}{\partial z}\bigg|_{z=0} = \tau_y \qquad \text{for} \quad 0 \leq x \leq L \tag{15}$$

$$A_V \frac{\partial v}{\partial z}\bigg|_{z=0} = 0 \qquad \text{for} \quad L < x < \infty$$

$$u = v = 0 \qquad \text{for } x = 0$$

$$u = v = 0 \qquad \text{for } z = -b$$

$$u = v = \frac{\partial \xi}{\partial x} = 0 \quad \text{for } x = \infty$$

These equations yield a rather complicated solution in terms of streamlines in the vertical plane perpendicular to the coast.

Hidaka defines a horizontal frictional distance, D_H, in analogy to Ekman's depth of frictional influence, D_v, given in equation (9).

$$D_H = \pi \sqrt{\frac{A_H}{\rho \omega \sin \varphi}} \tag{16}$$

For the case of a longshore wind, upwelling is shown to be confined to a strip of width less than 0.5 D_H, with sinking occurring at distances from the coast greater than D_H. A numerical example is considered with a wind stress τ_y = 1 c. g. s. unit and a wind zone of the order of 300 kilometers. Assuming $A_H = 10^9$ c. g. s. units and $A_v = 10^3$ c. g. s. units an upwelling velocity of 3×10^{-3} cm/sec is obtained. The width of the upwelling zone is about 80 kilometers. While the vertical velocity and width of upwelling are of the order of magnitude observed, the value assumed for A_H is extremely large. The values for the ocean are generally considered to range from 10^5 to 10^8 c. g. s. units. The higher values are found in the swift western boundary currents (1, p. 818). Sverdrup and Fleming (38, p. 341)

computed lateral eddy diffusion coefficients off southern California during the upwelling season and found values ranging from 10^6 to 10^7 c. g. s. units. Though these values are for horizontal eddy diffusivity, the coefficients of horizontal eddy viscosity and diffusivity appear to be equal (39, p. 483). McEwen (21, p. 201) calculated values for the the horizontal eddy viscosity off southern California and found values of the order of 10^5 c. g. s. units. Using even the relatively large value of $A_H = 10^7$ c. g. s. units as reasonable for the eastern boundary of the ocean, Hidaka's theory limits upwelling to less than 10 kilometers from the coast, and sinking beyond 20 kilometers. This is not in agreement with observations off the coast of Oregon or California. The theory also does not take into account density stratification which is observed to play a decisive role in the ocean (4, vol. 1, p. 653).

The Theory of Yoshida

Yoshida (52) has investigated theoretically the upwelling associated with winds of a week or longer duration. He considers a two layer ocean with a homogeneous upper layer of average thickness h. The density difference between the lower and upper layers is $\Delta\rho$. A straight coast is defined by $x = 0$. It is assumed there are no variations in conditions in the y-direction. The wind blows parallel to

$$-fv = -\frac{1}{\rho}\frac{\partial p}{\partial x}$$

$$fu = \frac{\tau_y}{\rho h} + \frac{A_H}{\rho}\frac{\partial^2 v}{\partial x^2} \qquad (21)$$

Assuming the eddy coefficients for mixing and viscosity are equal, one obtains from the continuity of concentration

$$w\frac{\partial \rho}{\partial z} = \frac{A_H}{\rho}\frac{\partial^2 \rho}{\partial x^2} \qquad (22)$$

Yoshida states that these equations will yield the same equation (19) for vertical velocity.

Defant (4, vol. 1, p. 656) feels that this approach provides deeper insight into the dynamics of upwelling. Besides predicting the vertical velocities it furnishes a characteristic width for upwelling which Yoshida takes as $L = \pi/k$. A very similar approach will be followed in obtaining a model for upwelling off the Oregon coast.

Open Ocean Upwelling

Upwelling is, in general, the result of the horizontal divergence of the surface layer. Continuity requires a vertical transport of subsurface water into the surface layer. The theories of upwelling discussed above have considered the upwelling resulting from a

one-sided divergence of the surface layer induced by a wind stress parallel to a coastal boundary. This upwelling is often referred to as coastal upwelling and it occurs only within 100 kilometers from the coast.

A spatial variation in the wind stress on the sea could also cause a horizontal divergence of the Ekman layer, resulting in upwelling. This process could occur in the open ocean, away from the influence of coastal boundaries. The term open ocean upwelling is used to distinguish this process from coastal upwelling. Open ocean upwelling and coastal upwelling are neither mutually exclusive nor necessarily independent.

Freeman (9), Stommel (35), and Yoshida and Mao (57) have considered the effect of a wind induced horizontal divergence on the surface layer. Yoshida and Mao were interested in upwelling of large horizontal extent off southern California and give the most complete study of open ocean upwelling.

Yoshida and Mao eliminated the pressure terms in equations (1) and (2) by cross-differentiation. The result, assuming density variations to be negligible, is the approximate vorticity equation (57, p. 41):

$$\frac{d}{dt}(\zeta+f) = -(\zeta+f)\left(\frac{\partial u}{\partial x}+\frac{\partial v}{\partial y}\right) + \frac{1}{\rho}\frac{\partial}{\partial z}\left(\frac{\partial \tau_{yz}}{\partial x}-\frac{\partial \tau_{xz}}{\partial y}\right) + \frac{A_H}{\rho}\left(\frac{\partial^2 \zeta}{\partial x^2}+\frac{\partial^2 \zeta}{\partial y^2}\right) \tag{23}$$

where ζ is the vertical component of the relative vorticity,

$$\zeta = \frac{\partial v}{\partial x} - \frac{\partial u}{\partial y}$$

and the vertical friction is represented by shearing stresses. The relative magnitudes of the terms are then considered, and only the higher order terms are kept. Using the equation of continuity (5), the simplified equation can be written

$$\rho \frac{\partial w}{\partial z} = \frac{\beta}{f} \rho v - \frac{1}{f} \frac{\partial}{\partial z} \left(\frac{\partial \tau_{yz}}{\partial x} - \frac{\partial \tau_{xz}}{\partial y} \right) \tag{24}$$

The vertical velocity at the surface vanishes and the stress is assumed negligible at the bottom of the surface or Ekman layer. Integrating the equation vertically from the base of the Ekman layer, - h, to the surface, one obtains:

$$\rho w_{-h} = \frac{1}{f} \left(\frac{\partial \tau_y}{\partial x} - \frac{\partial \tau_x}{\partial y} \right) - \frac{\beta}{f} \int_{-h}^{0} \rho v \, dz \tag{25}$$

The stress at the sea surface is set equal to the wind stress. The integral in the last term is the total transport in the surface layer: Ekman plus geostrophic.

Alternately one may integrate the equation (24) from the bottom of the sea, z = -b, to the base of the Ekman layer. The vertical velocity vanishes at the bottom and the stresses in the lower layers of the sea are considered negligible. One obtains then:

$$\rho w_{-h} = \frac{\beta}{f} \int_{-b}^{-h} \rho v \, dz \qquad (26)$$

The physical meaning is that the vertical motion at any depth below which the stresses can be neglected is proportional to the meridional transport below that depth. In both hemispheres the subsurface poleward transport of water is associated with ascending motion.

Equations (25) and (26) provide two ways of obtaining the vertical velocities in open ocean upwelling. Further assumptions must usually be made in order to evaluate the terms because the transports involved are total. If we can assume a level surface at some depth, say 1000 decibars, we can obtain the geostrophic transport above that level. With wind and hydrographic data it is then possible to find approximate values for the terms in the equations.

In applying the equation (25) to the ocean off southern California, Yoshida and Mao made the further assumption that the meridional transport in the surface layer is negligible (57, p. 44). This assumption reduces equation (25) to the form obtained by Freeman (9) since he considered no variation in the Coriolis parameter.

Yoshida and Mao find agreement between theory and observation off southern California (57, p. 47-51). They observe that the density at 150 meters increases from month to month, indicating upwelling,

when the curl of the wind stress is positive. They also find upwelling associated with subsurface meridional transport. The open ocean upwelling off southern California observed by Yoshida and Mao occurs from March to May - the same months coastal upwelling occurs inshore.

III. A MODEL OF UPWELLING FOR THE OREGON COAST

The oceanic area off the coast of Oregon will be considered as divided into two regions:

1). The region of coastal upwelling, extending less than 100 kilometers out from the coast.

2). The region further offshore where the effects of the coastal boundary may be ignored. Here open ocean upwelling may occur. This region, for the purpose of this study, can be considered to extend indefinitely.

The processes in the two regions will differ not only because of the presence or absence of the coastal boundary but also because of the vast difference in the scale or extent of the two regions. While the wind can be considered as constant over the coastal region, it cannot be over the 1000 kilometers of open ocean. Also, the variation of the Coriolis parameter with latitude should not be ignored in the open ocean region.

The density structure of the ocean off Oregon is taken to be three-layered. The surface or upper layer (the layer of frictional influence) is assumed homogeneous with density ρ_1, but of variable depth, h. Below this layer is the pycnocline, or frontal layer, in which the density changes by $\Delta\rho$ from ρ_1 of the upper layer to ρ_2 of the deep layer.

This is an idealized representation of the permanent density structure of the ocean off Oregon.

It is assumed that the homogeneous layer and the drift current layer coincide. In theory, the homogeneous layer, the layer of frictional influence, and the drift current layer coincide exactly in the steady state according to Rossby and Montgomery (33, p. 67). The effect of the pycnocline is, in any case, to reduce the vertical frictional transport of momentum to practically zero (43, p. 46). The vertical shearing stress thus effectively vanishes at the base of the surface layer and the drift current layer is limited to the homogeneous surface layer.

The Oregon coastline runs approximately along the meridian 124° west longitude. The coordinate system defined in Section II will be used in this model. The coastal boundary will be defined by the line $x = 0$. It is assumed that there are no variations in the conditions or parameters in the y-direction (the longshore direction) within a few hundred kilometers of the coast. This assumption is supported by observation.

The coastal and the offshore or open ocean regions will be treated separately. The condition will be imposed that the two solutions yield the same surface layer zonal mass transport at the boundary between the regions.

The Open Ocean Region

Observations show that away from the boundaries on the eastern sides of the oceans, accelerations are small and horizontal friction is negligible compared to vertical friction. The horizontal equations of motion in a form valid under these conditions are

$$-fv = -\frac{1}{\rho}\frac{\partial p}{\partial x} + \frac{1}{\rho}\frac{\partial \tau_{xz}}{\partial z} \tag{27}$$

$$fu = -\frac{1}{\rho}\frac{\partial p}{\partial y} + \frac{1}{\rho}\frac{\partial \tau_{yz}}{\partial z} \tag{28}$$

The vertical frictional forces are written explicitly as shearing stresses.

The pressure terms can be eliminated by cross-differentiation. Using the equation of continuity (5), one obtains

$$-\rho f\frac{\partial w}{\partial z} + \rho\beta v = \frac{\partial}{\partial z}\left(\frac{\partial \tau_{yz}}{\partial x} - \frac{\partial \tau_{xz}}{\partial y}\right) \tag{29}$$

The vertical velocity at the bottom of the surface layer is found by integrating vertically over the surface layer. Since the vertical velocity at the sea surface is zero and the stresses at the bottom of the surface layer are assumed to vanish, the following expression for the vertical velocity at the bottom of the surface layer is obtained:

$$\rho f w_{-h} = -\beta \int_{-h}^{\xi} \rho v \, dz + \frac{\partial \tau_y}{\partial x} - \frac{\partial \tau_x}{\partial y} \tag{30}$$

The shearing stress evaluated at the sea surface is equal to the wind stress. Using the first of the equations of motion (27), w_{-h} can be written

$$w_{-h} = -\frac{\beta}{f^2 \rho} \int_{-h}^{\xi} \frac{\partial p}{\partial x} \, dz + \frac{\beta}{f^2 \rho} \tau_x + \frac{1}{f \rho} \left(\frac{\partial \tau_y}{\partial x} - \frac{\partial \tau_x}{\partial y} \right) \tag{31}$$

It will be required that the zonal mass transport out of the region of coastal upwelling equal the offshore transport in the open ocean region in the vicinity of the boundary between regions. Since variations in the y-direction are assumed negligible within a few hundred kilometers of the coast, the pressure term in equation (28) may be neglected there. The zonal mass transport in the open ocean in the vicinity of the boundary between the open ocean and the coastal region can be found by integrating this simplified equation over the surface layer. Again, the stress at the sea surface is equal to the component of the wind stress and the stress at the lower limit is assumed to vanish. The vertical integration yields

$$M_x = \int_{-h}^{\xi} \rho u \, dz = \frac{\tau_y}{f} \tag{32}$$

This is simply the zonal component of the Ekman transport.

Coastal Upwelling

The general approach in the coastal region will be similar to that of Yoshida (52), though differing in detail and specialized to the Oregon coast.

The horizontal equations of motion and the equation of continuity for the surface layer of the coastal region are used in the following form:

$$0 = fv - g\frac{\partial \xi}{\partial x} + \frac{1}{\rho}\frac{\partial \tau_{xz}}{\partial z} \tag{33}$$

$$\frac{\partial v}{\partial t} = -fu + \frac{1}{\rho}\frac{\partial \tau_{yz}}{\partial z} + \frac{A_H}{\rho}\frac{\partial^2 v}{\partial x^2} \tag{34}$$

$$0 = \frac{\partial u}{\partial x} + \frac{\partial w}{\partial z} \tag{35}$$

The pressure gradients in the homogeneous surface layer are represented by the slope of the sea surface. Vertical friction is represented by shearing stress and lateral friction by the horizontal eddy viscosity and lateral velocity gradient.

Processes extending over several days to several weeks are considered. The equations are held to apply after the wind has been

blowing steadily for a day or so and the drift currents have been established. The drift currents become practically fully developed within a day (5, p. 16). The acceleration in the x-direction is principally wind driven and can be neglected after the drift current is established. This is in agreement with observation.

Isostatic equilibrium is assumed to occur; the slope of the sea surface and the slope of the pycnoline layer will establish an isostatic condition in the deep layer. This compensation principle between the surface and deep layers in the ocean is confirmed by experience and is, according to Defant (4, vol. 1, p. 704), one of the most important experimental facts of oceanography. Yoshida (52, p. 11) quotes Defant as estimating that this adjustment occurs within a day or two off the California coast. The relation between the surface slope and the slope of the pycnocline layer, assuming isostatic adjustment is approximately:

$$\rho_1 g \frac{\partial \xi}{\partial x} = -g \Delta\rho \frac{\partial h}{\partial x} \tag{36}$$

Considering density as essentially a function of temperature and salinity, the equation of conservation of concentration (4,vol. 1, p. 105) is applied to density in the region of the pycnocline:

$$\frac{\partial \rho}{\partial t} + w \frac{\partial \rho}{\partial z} = \frac{A_H}{\rho} \frac{\partial^2 \rho}{\partial x^2} \tag{37}$$

The horizontal eddy diffusivity is considered constant and equal to the horizontal eddy viscosity. This appears to be true from the evidence available (39, p. 483).

In view of the density stratification, equation (37) can be written approximately in terms of the depth of the pycnocline layer (54,p.106):

$$w_{-h} = \frac{\partial h}{\partial t} - \frac{A_H}{\rho} \frac{\partial^2 h}{\partial x^2} \tag{38}$$

Essentially, the vertical advection of density is balanced by the uplift of the pycnocline layer and lateral mixing across the pycnocline. In the earlier stages of upwelling it is to be expected that the rate of ascent of the pycnocline approximates closely the vertical velocity. In the later or equilibrium stage when the pycnocline is approximately stationary, lateral mixing balances the vertical advection.

Using the isostatic relation, equation (38) can be written in terms of the surface elevation:

$$w_{-h} = \frac{\rho}{\Delta\rho} \left(\frac{A_H}{\rho} \frac{\partial^2 \xi}{\partial x^2} - \frac{\partial \xi}{\partial t} \right) \tag{39}$$

An equation for the vertical velocity at the bottom of the surface layer in the coastal region can be obtained from the equations of motion and the above relation. Solving equation (33) for v and substituting into equation (34), one obtains

$$\frac{\rho\beta}{f}\frac{\partial^2\xi}{\partial t\partial x} = -\rho f u + \frac{\partial\tau_{yz}}{\partial z} + \frac{\rho g}{f}\left(\frac{A_H}{\rho}\right)\frac{\partial^3\xi}{\partial x^3} - \frac{A_H}{\rho}\frac{1}{f}\frac{\partial^3\tau_{xz}}{\partial x^2\partial z} + \frac{1}{f}\frac{\partial^2\tau_{xz}}{\partial z\partial t} \tag{40}$$

The partial differentiation with respect to x yields, upon application of the equation of continuity and rearrangement of terms:

$$\frac{\rho g}{f}\frac{\partial^2}{\partial x^2}\left(\frac{\partial\xi}{\partial t} - \frac{A_H}{\rho}\frac{\partial^2\xi}{\partial x^2}\right) = \rho f\frac{\partial w}{\partial z} + \frac{\partial}{\partial z}\left(\frac{\partial\tau_{yz}}{\partial x}\right) + \frac{\partial}{\partial z}\left(-\frac{A_H}{\rho f}\frac{\partial^3\tau_{xz}}{\partial x^3} + \frac{1}{f}\frac{\partial^2\tau_{xz}}{\partial x\partial t}\right) \tag{41}$$

Again, the vertical velocity at the sea surface is zero and the stress at the bottom of the surface layer is assumed to vanish. Thus, vertical integration of equation (41) over the surface layer yields

$$\frac{\rho g h}{f}\frac{\partial^2}{\partial x^2}\left(\frac{\partial\xi}{\partial t} - \frac{A_H}{\rho}\frac{\partial^2\xi}{\partial x^2}\right) = -\rho f w_{-h} + \frac{\partial\tau_y}{\partial x} - \frac{A_H}{\rho}\frac{\partial^3\tau_x}{\partial x^3} + \frac{1}{f}\frac{\partial^2\tau_x}{\partial x\partial t} \tag{42}$$

The stress components evaluated at the sea surface are set equal to the wind stress components. The assumption is made that the wind is

approximately constant over the coastal region. Applying this assumption and equation (39) to equation (42) yields the following equation for w_{-h}

$$\frac{\partial^2 w_{-h}}{\partial x^2} - k^2 w_{-h} = 0 \qquad \text{where } k^2 = \frac{f^2}{\frac{\Delta\rho}{\rho_1} g h} \tag{43}$$

The parameter k is determined by the latitude and the density structure. The value of k will be taken as constant. This assumes, following Yoshida (52, p. 15), that an average depth of the surface layer can be used in the expression for k. The resulting mathematical simplicity allows comparison between the model and the data available.

The solution to equation (43) is immediate:

$$w_{-h} = A e^{kx} + B e^{-kx} \tag{44}$$

The second term on the right is discarded as physically unrealistic. The coefficient A can be evaluated by applying the boundary conditions for zonal mass transport.

Integrating the equation of continuity (35) vertically over the surface layer yields

$$\int_{-h}^{\xi} \rho \frac{\partial u}{\partial x} dz = -\int_{-h}^{\xi} \rho \frac{\partial w}{\partial z} dz = \rho w_{-h} \tag{45}$$

since the vertical velocity at the sea surface vanishes. The additional terms resulting from interchanging the order of integration and differentiation according to Leibnitz' rule are neglected, since the surface slope is small and the horizontal velocity is assumed to vanish at the bottom of the surface layer, yielding

$$\frac{dM_x}{dx} = \frac{d}{dx}\int_{-h}^{\xi} \rho u \, dz = \rho w_{-h} \tag{46}$$

Integrating the above equation with respect to x from the coast, x = 0, out to a distance x =-L, the outer limit of the coastal upwelling region, yields:

$$M_x\Big|_{x=-L} - M_x\Big|_{x=0} = \int_0^{-L} \rho A e^{kx} dx = \rho \frac{A}{k} e^{-kL} - \rho \frac{A}{k} \tag{47}$$

The zonal mass transport evaluated at x = 0 must be zero since there can be no mass transport through the coastal boundary. The zonal mass transport at the outer edge of the coastal upwelling region, x =-L, must equal the transport obtained for the inner portion of the open ocean region, as given by equation (32). The term in equation (45) involving e^{-kL} can be neglected since L is of the order of 100 kilometers and any realistic evaluation of k shows it to be of the order of 10^{-6} cm^{-1}. Solving for A yields

$$A = -\frac{k}{\rho}\frac{\tau_y}{f}$$

Thus, the vertical velocity at the bottom of the surface layer in the coastal region is given by

$$w_{-h} = -\frac{k}{\rho f} \tau_y e^{kx} \tag{48}$$

In summary: The model of upwelling for the Oregon coast provides expressions for the vertical velocity at the bottom of the surface layer for both open ocean and coastal upwelling in equations (31) and (48) respectively. The amount of water upwelled through the bottom of the surface layer per unit meridional length in a unit time in the coastal region is given by:

$$\int_{-L}^{0} \rho w_{-h} \, dx = -\frac{\tau_y}{f} \tag{49}$$

The effective width of the coastal upwelling belt is given through the parameter k, equation (43).

IV. THE DATA

Wind Stress

The most important single parameter in upwelling is the stress exerted by the wind on the sea surface. Indeed, in any consideration of ocean movements, from ripples on the surface to large scale permanent ocean currents, wind stress is a major factor. It is important to obtain a reliable estimate of the wind stress to discuss upwelling quantitatively or to test the validity of a model.

Momentum is exchanged between the atmospheric and oceanic circulation by means of shearing stress. The shearing stress in a fluid is in general a symmetric tensor. The τ_{xz} and τ_{yz} components are of particular interest. These components evaluated at the sea surface equal the components of the stress exerted by the wind on the sea, or the transfer of horizontal momentum vertically across the air-sea interface.

The stress of the wind on the sea cannot be measured directly but can be computed by several indirect methods. The only method, however, that has proved suitable for systematic determinations is based on the formula giving the wind stress on the sea surface, $\vec{\tau}$, in terms of the air density, ρ_a, a dimensionless drag coefficent, C_D, and the wind velocity, $\vec{u}_a$, measured at a distance, a, (usually 10 meters) above the sea surface.

$$\vec{\tau} = \rho_a C_D |\vec{u}_a| \vec{u}_a \qquad (50)$$

This formula has been used in virtually all circulation dynamics studies. It can be deduced by dimensional reasoning. It can also be deduced from observation, as done by Ekman (5, p. 40), or obtained from classical turbulence studies such as those of Rossby and Montgomery (33, p. 5-6).

Many determinations, from various approaches, have been made to determine the drag coefficent, C_D, which was first defined by Taylor (41). In general, C_D is a function of other dimensionless parameters involving wind speed, surface roughness, height of wind measurement and stability of air over the sea. There is evidence to indicate the existence of a critical wind speed below which the sea surface is hydrodynamically smooth and above which it is rough, leading to different values for C_D. Munk (24, p. 212) shows the critical wind speed to be between six and eight m/sec. Above this wind speed C_D appears to be constant, but below this speed the value is only approximately constant.

Wilson (45) has reviewed all available literature of laboratory and field measurements of C_D and adjusted them to prototype conditions at 10 meters height. The values for the dimensionless drag coefficent for strong and light winds are $0.0024 \pm .0005$ and $0.0015 \pm .0008$ respectively. Wilson does not specify his definition for strong and

light winds but it appears that the dividing point is about 15 knots, corresponding closely to Munk's critical wind speed. Sverdrup (36, p. 628) had previously suggested using the value of 2.4×10^{-3} as the best estimate of C_D, particularly if the wind speed varies over a wide range. This is reasonable because the stress values for low wind speeds enter with small weight only, since the stress is proportional to the square of the wind speed.

The procedure used in this study is to use the value 2.4×10^{-3} for C_D with mean winds, but to use Wilson's two values where individual wind velocity measurements were available.

The uncertainties in regard to the validity of equation (50) and the value for C_D are, unfortunately, not the least of the uncertainties in obtaining a mean wind stress. Ideally, one would need a dense distribution of oceanic stations reporting the wind accurately many times a day. From each observation of the wind velocity, the components of the surface wind stress could be computed. The two components could be averaged individually to find the mean wind stress vector. In general, this would give a stress different in direction and magnitude from the stress computed from the more readily available mean resultant wind. The two values would be equal only for a wind steady in velocity. Since a completely random wind velocity distribution would give a mean resultant wind close to zero, it is to be expected that the stress computations based on the mean resultant wind will underestimate the magnitude of the mean wind stress.

The major atmospheric circulation is fairly regular, although varying seasonally in many areas. It is thus possible to obtain an approximation to the monthly mean wind stress from the monthly mean sea level pressure charts. The monthly mean sea level pressure charts yield a mean resultant wind through the geostrophic computations (6, p. 29-33).

Another source of climatic wind data is contained in the Pilot Charts. The charts contain wind roses giving the average distribution over a given time and region. The wind roses give the percentage of time the wind blows from each of the 16 points of the compass and the mean wind speed for that direction. Workers at Scripps Institution of Oceanography evaluated the mean wind stress for five degree quadrangles in the North Pacific for each month (34). They obtained a wind speed distribution function for each mean wind speed from climatic charts and thus obtained a mean wind stress for each point of the compass. Finally, a frequency weighted resultant mean wind stress was obtained.

Malkmus (17, p. 187-189) has compared the mean wind stress vector obtained from the several methods using data obtained during

oceanographic cruises. The results are in surprising agreement, the agreement being roughly proportional to the wind steadiness.

The Meterorological Data

The wind data available for obtaining a value of the wind stress in the vicinity of the Oregon coast are fourfold:

1). The monthly mean wind stress charts computed at Scripps Institution of Oceanography (34). These values were derived from the pilot charts, which show average winds from many years of ship reports, weighted to yield resultant wind stress. Data of this kind have been used by Wyrtki in his study of upwelling off Peru (51, p. 316) and by Reid and Wooster (47, p. 267-268) in a qualitative discussion of upwelling along the western coasts of the continents.

2). The monthly mean sea level pressure charts issued by the Extended Forecast Section of the United States Weather Bureau. These charts were obtained through the courtesy of Jerome Namias, Chief of the Extended Forecast Section. The monthly means of the sea level atmospheric pressure at a regular set of grid points are obtained from averaging twice daily observations. One may then obtain the mean resultant geostrophic wind and hence an estimate of the mean wind stress for each month of each year. Data of this type have been used by Montgomery (23) in his study of the transport of the surface

water in the North Atlantic and by Fofonoff (7, 8) in his extensive study of mass transport in the North Atlantic and North Pacific. The mean wind stress at 125° west longitude and 45° north latitude (approximately 40 nautical miles off Newport, Oregon) has been computed using the monthly mean pressure charts for each month from 1960 through 1963.

3). The sea level pressure charts received several times daily from the U.S. Weather Bureau on the facsimile equipment of the Physics Department of Oregon State University. The data are given as pressure contours. The geostrophic wind at the point of interest can be computed from each chart. The wind stress can then be obtained and the components of the stress average over the period desired. This involves considerable work and some subjective error to obtain averages over extended periods. This source of mean wind stress was used for short periods and as an occasional check on the monthly mean wind stress found from the monthly mean sea level pressure charts.

4). The wind velocities obtained from shipboard observations. This would provide a good estimate of the mean wind stress if sufficient ships took a sufficient number of observations. Montgomery (23) concluded from his study that the winds computed from pressure gradients are not only more consistent and easier to handle, but more accurate if observations are meager. This is because a relatively

few ships can define the pressure system over the ocean with fair accuracy, while many more ships would be needed to define the wind system.

All four of the above sources of wind data have been used in this thesis. For an estimate of the mean wind stress during the period between the monthly or bi-monthly oceanographic cruises of Oregon State University, the monthly mean pressure charts were used. The wind velocity at 10 meters was obtained by first computing the mean resultant geostrophic velocity. The geostrophic velocity was then rotated by 15 degrees to the left of the downwind direction and reduced to 70 % of its magnitude to estimate the surface (10 meters) wind velocity. This follows the procedure used by Fofonoff (8, p. 1) Montgomery (23) and Sverdrup and Fleming (38, p. 319-320) used similar procedures to obtain the surface wind from the geostrophic wind, although slightly different values for the angle and attenuation were used in each case.

For shorter term mean wind stress the daily pressure charts and shipboard observations were used. The same procedure as mentioned in the above paragraph was used to obtain surface winds from the geostrophic winds computed from daily pressure charts. When shipboard observations of the wind were used, a selection of observations

separated by approximately equal time intervals was made. To obtain the mean wind stress from these sources, the two components of the wind stress from each observation were averaged separately.

In the model proposed for the Oregon coast, and essentially in all theories of coastal upwelling, the component of the wind stress vector parallel to the coast is the significant parameter. In the case of the Oregon coast, the component of the wind stress causing the coastal upwelling is τ_y, the north-south component. The monthly mean of this component off the Oregon coast is shown in Figure 1 for the period from June 1961 to September 1963. The wind stress was computed from the monthly mean pressure charts for 125° west latitude and 45° north latitude.

The 14 year average (1950-1963) of the monthly means of τ_y is shown in Figure 2. The standard deviations varied from 0.09 dynes/cm^2 for July to 0.60 dynes/cm^2 for January. Also shown in Figure 2 is the τ_y component of the resultant mean wind stress computed for the same area at the Scripps Institution of Oceanography (34). The values in the two oceanic quadrangles having the common point 125° west longitude and 45° north latitude were averaged to obtain the latter values.

The agreement between the two sets of points in Figure 2 is as good as can be expected. The only disagreement as to direction

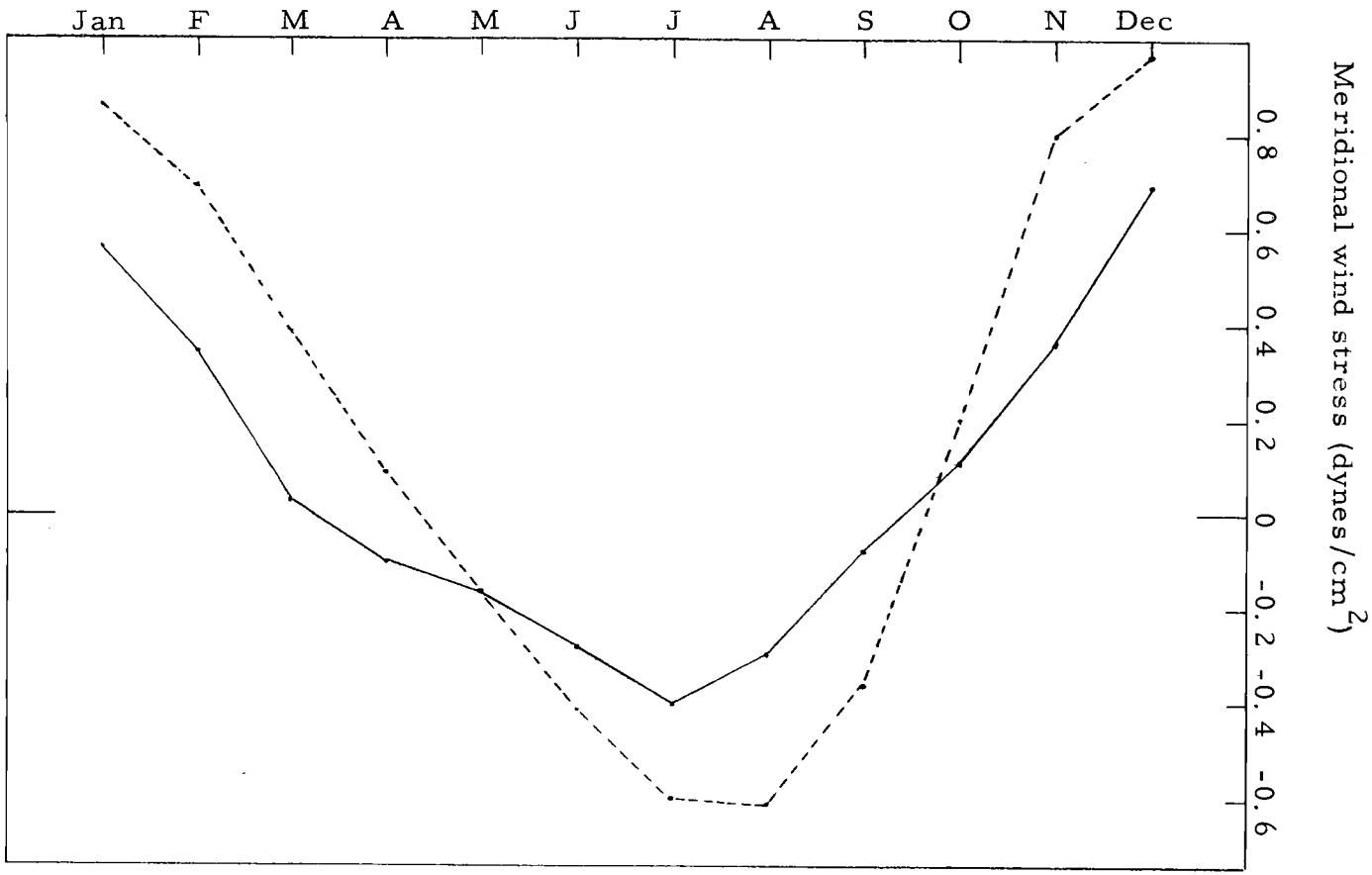

Figure 2. Fourteen-year average of monthly meridional wind stress component at 45°N, 125°W computed from monthly mean pressure charts (solid line) and monthly mean meridional component of resultant wind stress from pilot charts (34)(dashed line).

occurs in April. April, however, has a very high standard deviation. The expectation is borne out that the mean stress computed from the resultant wind (obtained from the monthly mean charts) would be less than that of the resultant stress itself.

An estimate of the wind steadiness off the Oregon coast can be obtained from the United States Weather Bureau Climatic Charts of the Oceans(42). The constancy parameter given in the charts is the percentage of winds in the same quadrant as the resultant wind. The constancy off the Oregon coast is high (61% to 80%) for the upwelling season (May to September). Confidence can thus be placed in the wind stress values obtained from the resultant wind during the upwelling period.

The Oceanographic Data

The model of upwelling for the Oregon coast provides an expression for the vertical velocity at the bottom of the surface or drift current layer. The vertical velocity is in general a function of the wind stress and oceanographic parameters. The meteorological data have been discussed in the preceding part. The oceanographic data used in this study were obtained from the oceanographic cruises of Oregon State University. Since May 1961 regular hydrographic cruises have been made by Oceanography Department personnel abroad the

R/V ACONA. Prior to May 1961 hydrographic cruises were made on a less regular basis aboard charter vessels.

This study covers the period from September 1960 to September 1963 inclusive. Attention was concentrated on the section off Newport ($44^{o}39'$ north latitude) and off Brookings ($42^{o}00'$ north latitude). The Newport section is considered typical of the general features of the ocean off Oregon. It also provides the largest and most complete set of data since the hydrographic stations were occupied on a monthly or bi-monthly basis. The Brookings section provides additional data on coastal upwelling since it transects an area of pronounced coastal upwelling.

The hydrographic data consist of temperature and salinity observations at given depths at a regular set of stations off the coast. Stations are occupied every 10 nautical miles starting from five miles off the coast to 45 nautical miles off the coast and thereafter every 20 nautical miles out to 165 nautical miles from the coast. The temperature and salinity values at standard depths are interpolated by a modified parabolic procedure. The density is computed at the standard depths and is given in terms of sigma-t, σ_t . From these data other parameters of interest are computed, e.g. the geopotential anomalies for geostrophic current calculations. The hydrographic data provide knowledge of the density structure of the ocean off the

Oregon coast and the values for the oceanographic parameters in the model.

In the case of coastal upwelling, the depth of the surface layer and the density difference between the surface and the deep layer enter as the oceanographic parameters. In the model the surface layer is taken to be a homogeneous layer of uniform density. In the real ocean there seldom is a truly homogeneous layer of appreciable depth. In studies where the density structure of the ocean is approximated by a two layer model, the surface layer is usually taken to extend down to the depth of greatest density gradient (56). In the three-layer model for the ocean off Oregon, the intermediate layer is the region of rapid density change with depth. This layer corresponds to the observed front or pycnocline, the layer in which the change density with depth is noticeably greater than in the layers above and below. An example of the observed density structure is shown in Figure 3. The pycnocline or oceanic front off the Oregon coast has been studied by Collins (2). He found that the 25.5 and 26.0 sigma-t surfaces (density 1.0255 and 1.0260 gr/cm^3) were always within the pycnocline. Collins chose these two sigma-t values to delineate the front (2, p. 17). In the present study, the 25.5 sigma-t surface was accordingly chosen as the bottom of the surface layer.

The depths of the 25.5 and 26.0 sigma-t values were computed

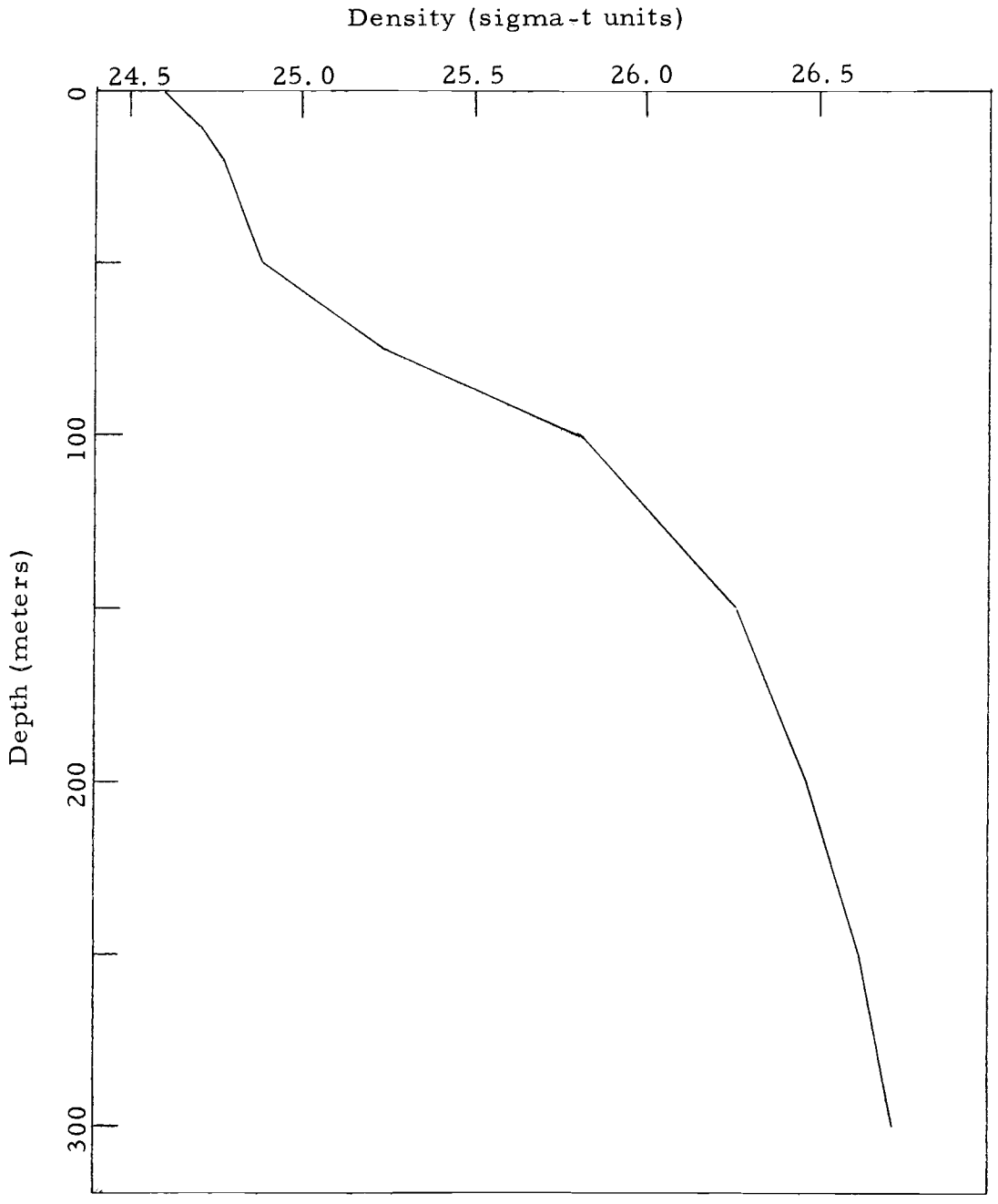

Figure 3. Density versus depth 45 nautical miles off the coast at 42°N in May 1963.

for all stations from the hydrographic data. The computer program, written by Mrs. Sue Borden, obtained the depth of the sigma-t values by linear interpolation of the observed hydrographic data. By using the observed hydrographic data rather than that already interpolated to standard depths, interpolation upon interpolations was avoided. Under the assumption that no velocity gradients exist in the longshore direction and that mixing across the sigma-t surfaces is negligible, the change in the depth of the isopycnals between cruises gives an estimate of the vertical velocities. Futhermore, since in this model the surface layer is assumed to coincide with the drift current layer, the integral of the vertical velocity of the 25.5 sigma-t surface from the coast out to the edge of the coastal region should provide an estimate of the offshore transport.

A density value representative of the surface layer can be found by averaging the hydrographic data, weighted according to depth intervals. In general the mean density of the surface layer (the layer above the depth of sigma-t equal to 25.5) would be found to be 24.5 ± 0.5 sigma-t units. The density below the pycnocline increases very slowly with depth from a value of about 26.2 sigma-t units at the base of the pycnocline. A characteristic value of the density at 200 meters (always below the pycnocline) would be 26.5 sigma-t units. Thus a representative value for $\Delta\rho$ in the model would be 2×10^{-3}

gm/cm^3. Since $\Delta\rho$ enters only as the square root, small variations in its value do not materially affect the results. $\Delta\rho$ was considered to have the constant value 2×10^{-3} in the model.

V. RESULTS

Open Ocean Upwelling

The equation for the vertical velocity at the bottom of the surface layer for the open ocean region of the model is given by equation (31)

$$w_{-h} = \frac{1}{f\rho}\left(\frac{\partial \tau_y}{\partial x} - \frac{\partial \tau_x}{\partial y}\right) + \frac{\beta}{f^2\rho}\tau_x - \frac{\beta}{f^2\rho}\int_{-h}^{\xi} \frac{\partial p}{\partial x}\, dz \,.$$

The first term on the right is the horizontal divergence in the surface layer caused by spatial variation in the wind stress or, in other words, the curl of the wind stress. The second and third terms on the right are the horizontal divergence exhibited by the meridional Ekman and geostrophic transports respectively. The evaluation of the parameters involved in open ocean upwelling is more difficult than in the case of coastal upwelling. The vertical velocities are at least an order of magnitude smaller than in the case of coastal upwelling. The wind stress must be known with enough precision at several locations to be able to estimate the curl of the wind stress. Finally, the meridional transport in the surface layer must be obtained.

The best estimate of the monthly mean curl of the wind stress off Oregon is probably to be obtained from the monthly mean wind stress charts made at the Scripps Institution of Oceanography (34). The

value of the curl was found for 45° north latitude, 130° west longitude from the mean wind stress in the four five-degree quadrangles about this point. The monthly values of the wind stress curl are given in Table 1.

Table 1. Wind stress curl at 45° north latitude, 130° west longitude

Month	Curl 10^{-9} dynes/cm^3	Month	Curl 10^{-9} dynes/cm^3
January	21.0	July	- 9.0
February	21.0	August	- 9.0
March	10.0	September	- 5.0
April	2.0	October	0
May	- 3.0	November	5.0
June	- 5.0	December	13.0

The values for the east-west component of the wind stress, τ_x, entering into the equation (31) were obtained from the same chart, but the magnitudes were always less than 0.4 dynes/cm^2. Therefore, the contribution of the meridional Ekman transport in the equation for open ocean upwelling is an order of magnitude less than the effect of the curl of the wind stress and is therefore neglected.

The meridional geostrophic transports were computed using standard oceanographic methods (36, p. 650-652) from the geopotential

anomalies obtained from hydrographic data. The transports through the sections 65 to 105 and 105 to 145 nautical miles from the coast at 44°39' north latitude were computed relative to the 1000 decibar level. The transports given in Table 2 are the net meridional geostrophic transports in the layer 0 to 100 meters relative to 1000 decibars. For the purposes of geostrophic computation the surface layer has been taken to be 100 meters thick in the open ocean off Oregon. This assumption is common for the mid-latitudes (51, p. 313) and in accord with existing data. The average depth of the 25.5 sigma-t surface, the assumed bottom of the surface layer in the model, is 85 meters at 125 nautical miles off the coast. Any discrepancy caused by this inconsistency should be negligible.

It was apparent from the hydrographic data that the effect of the coastal upwelled water being transported offshore was present out to 85 nautical miles from the coast. This is reflected in the increased southerly transport through the section 65 to 105 nautical miles off the coast during the upwelling season. The increase is due to the accumulation of denser water inshore and the concommitant lowering of the sea level, increasing the horizontal pressure gradient. This increased transport was also observed by Sverdrup and Fleming (38, p. 273-275) off southern California during coastal upwelling. For the discussion of open ocean upwelling it was therefore advisable to

Table 2. Surface layer meridional geostrophic transports through sections along 44° 39' north latitude.

Date	Transport through section 65-105 nautical miles from the coast	Transport through section 105-145 nautical miles from the coast
	10^{12} gr/sec	10^{12} gr/sec
June 1961	-0.37	-0.72
October 1961	+0.25	-0.22
December 1961	-0.24	+0.07
June 1962	+0.01	+0.11
July 1962	-0.73	+0.21
September 1962	-0.59	0
December 1962	+0.17	-0.07
February 1963	-0.10	-0.08
May 1963	+0.06	+0.09
September 1963	-0.12	+0.05

restrict the discussion to the section further offshore.

The geopotential anomalies, from which the geostrophic transports are computed, are uncertain to 0.01 dynamic meters (4, vol. 1, p. 311;48, p. 564). This results in an uncertainty of 0.1×10^{12} gr/sec in the geostrophic transport in the upper 100 meters through the sections. It is apparent from the values of the geostrophic transports in Table 2 that the magnitudes are usually about the same size as the uncertainty. This is not surprising for a section of this size since the eastern boundary currents are broad and slow. The magnitudes are too small to contribute appreciably to the equation for open ocean upwelling, and may be neglected. This reduces equation (31) for open ocean upwelling off the Oregon coast to a function of the wind stress curl alone.

In Section II, Open Ocean Upwelling, an alternate expression for open ocean upwelling was obtained in equation (26). It was observed that the vertical motion at any depth below which the stress vanishes is proportional to the meridional mass transport below that depth. Subsurface poleward mass transport is associated with ascending motion. Equation (26) can thus be used to estimate the vertical velocity at the bottom of the surface layer in the open ocean region.

$$w_{-h} = \frac{\beta}{\rho f^2} \int_{-b}^{-h} \frac{\partial p}{\partial x} dz$$

Below the surface layer, the stresses vanish and it is usually assumed that transports are approximately geostrophic. Assuming a level surface at 1000 decibars, the meridional geostrophic mass transport from 100 meters to 1000 meters was computed for the two sections, 65 to 105 and 105 to 145 nautical miles from the coast at 44°39' north latitude. The values are given in Table 3. The uncertainity in the hydrographic data leads to an uncertainty of about 1.0×10^{12} gr/sec in this subsurface meridional mass transport. Again, the magnitude of the computed transports is of the same order as the uncertainty in the values. Off the Oregon coast it appears that such computations do not give definitive results. The best estimate for the open ocean upwelling is thus obtained from the wind stress curl.

To obtain an estimate of the vertical velocities one can note the changes in the depth of the sigma-t surfaces. Due to the small size of the changes relative to the uncertainties, only a qualitative comparison of the vertical velocity and the wind stress curl is justified. The data available were divided into periods during which the wind stress curl was significantly negative or positive - the months June,

Table 3. Subsurface (100 to 1000 meters depth) meridional geostrophic transports through sections along 44° 39' north latitude.

Date	Transport through section 65-105 nautical miles from the coast 10^{12} gr/sec	Transport through section 105-145 nautical miles from the coast 10^{12} gr/sec
June 1961	-0.7	-1.9
October 1961	-2.0	-0.8
December 1961	-2.1	+1.1
June 1962	+0.6	+0.3
July 1962	-0.6	+0.2
September 1962	+0.4	+1.1
December 1962	+1.3	-2.2
February 1963	+0.5	+0.7
May 1963	-0.5	+1.0
September 1963	+2.7	+0.3

July, August and September, and the months Novermber, December, January and February respectively. The vertical velocities obtained using the mean curl for the two periods are -0.7×10^{-4} cm/sec (downwelling) and 1.5×10^{-4} cm/sec (upwelling) respectively. The mean depths of the 25.5 sigma-t surface for the three outermost stations (125, 145 and 165 nautical miles from the coast) were averaged together for each of the periods. The mean depth during the negative curl period (downwelling) was 88 ± 3 meters, and during the period of positive curl (upwelling) it was 79 ± 3 meters. The mean depth of the 25.5 sigma-t surface over all months was 84 ± 2 meters.

There is thus qualitative agreement with the curl of the wind stress and the depth of the 25.5 sigma-t surface. As a negative result it can be said that if there is open ocean upwelling off Oregon it is weak and occurs at a different time than coastal upwelling. This is in contrast to the situation Yoshida and Mao (57, p. 51) observed off southern California where both forms of upwelling occured in the spring.

Coastal Upwelling

The model's validity should be most readily ascertained in the relatively early stages of upwelling. The pycnocline is then fairly level and horizontal mixing across the pycnocline would be at a

minimum. Thus the rate of rise of the 25.5 sigma-t surface should closely approximate the average vertical velocity at that surface.

Almost without exception studies of upwelling have been based on hydrographic observations from more or less regularly scheduled hydrographic cruises at monthly or longer intervals. This type of data forms the bulk of this study and essentially tests the model on a monthly average basis. However, a shorter term set of observations during relatively strong and steady winds provided a more direct comparison between the wind stress and the ocean's response, and hence a good test of the model.

The R/V ACONA was at the right place at the right time to observe the beginning of the upwelling season in May 1963. A set of observations of the early stages of coastal upwelling was obtained. The ship was operating off the southern coast of Oregon. The weather maps indicate winds in the area had been blowing from a southerly direction until about 10 May. The winds then became variable but with a resultant northerly component. After 13 May and until the ship left the area the winds had a persistent moderate to strong northerly component.

The R/V ACONA made two series of standard hydrographic casts along the Brookings line (42°00' north latitude) at distances 5, 15, 25 and 35 nautical miles from the coast. The two series were initiated

at the same phase of the tide (high) on 14 May and 17 May. The actual time between observations at a given station is nearly constant at 76 hours. The distribution of temperature and salinity at the two times is shown in Figures 4 and 5. Two additional series of stations run 10 minutes of latitude north and south of the Brookings line indicated negligible meridional gradients. The evidence is that there is ascending motion and transport of water offshore. This is precisely what we have defined to be upwelling. It is to be noted that the sloping isograms indicate that upwelling had already begun when the first set of observations were made. This is consistent with the fact that the mean wind stress in the four days proceeding the first observations was conducive to coastal upwelling.

Vertical velocities can be estimated from the vertical displacements of the isograms. The offshore velocity component can then be found from the equation of continuity, assuming no latitudinal velocity gradient. The offshore transport can be found by a slightly different means. Assuming no cross-isogram flow, one can interpret the change in the area between two isograms in the time between the two series as a zonal transport per unit meridional length. This can be done for each section defined by the coast and a station, and can be done independently for temperature and salinity. The data were analyzed in this manner by June Pattullo and Norman Kujala (26).

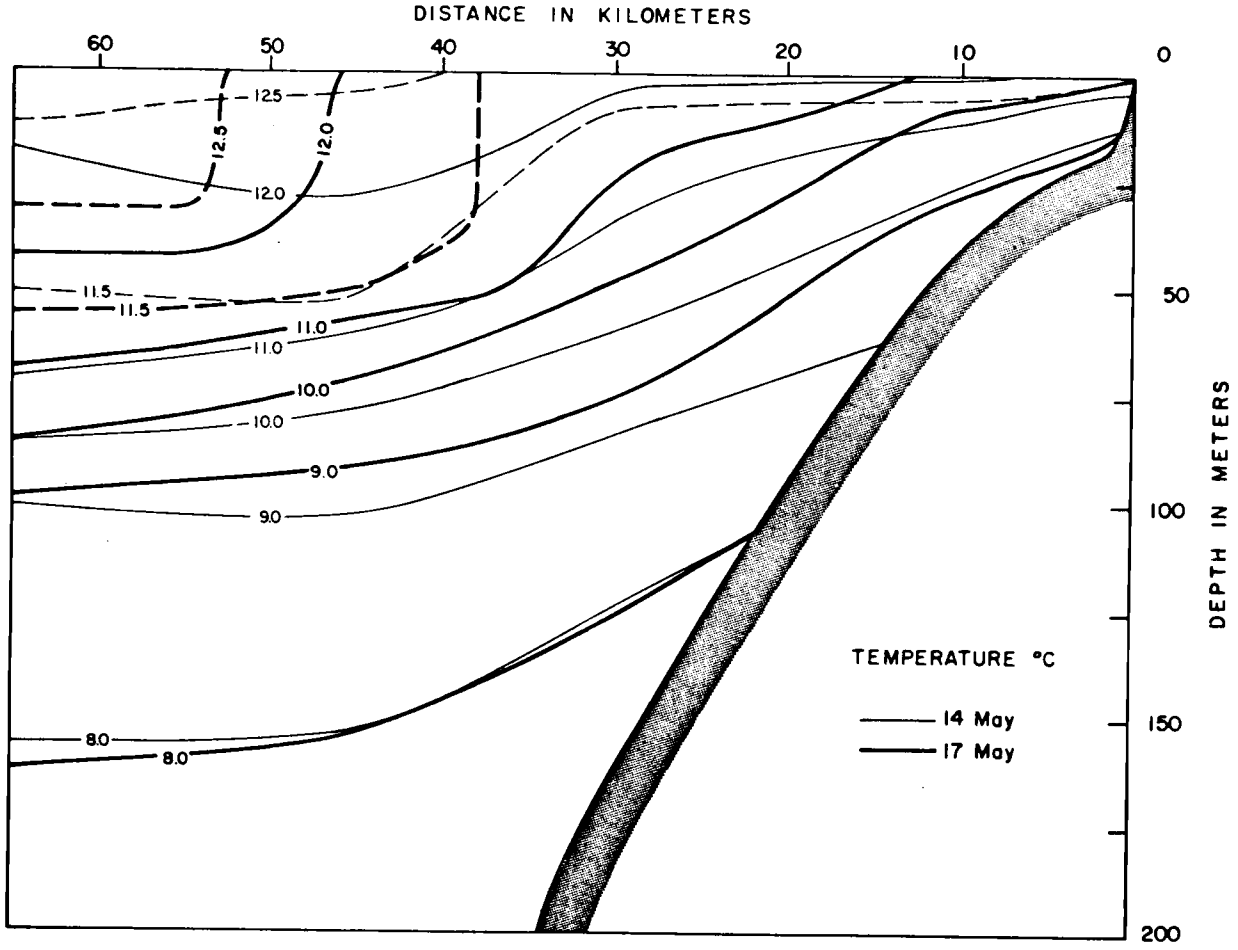

Figure 4. Temperature distribution along Brookings line in May 1963.

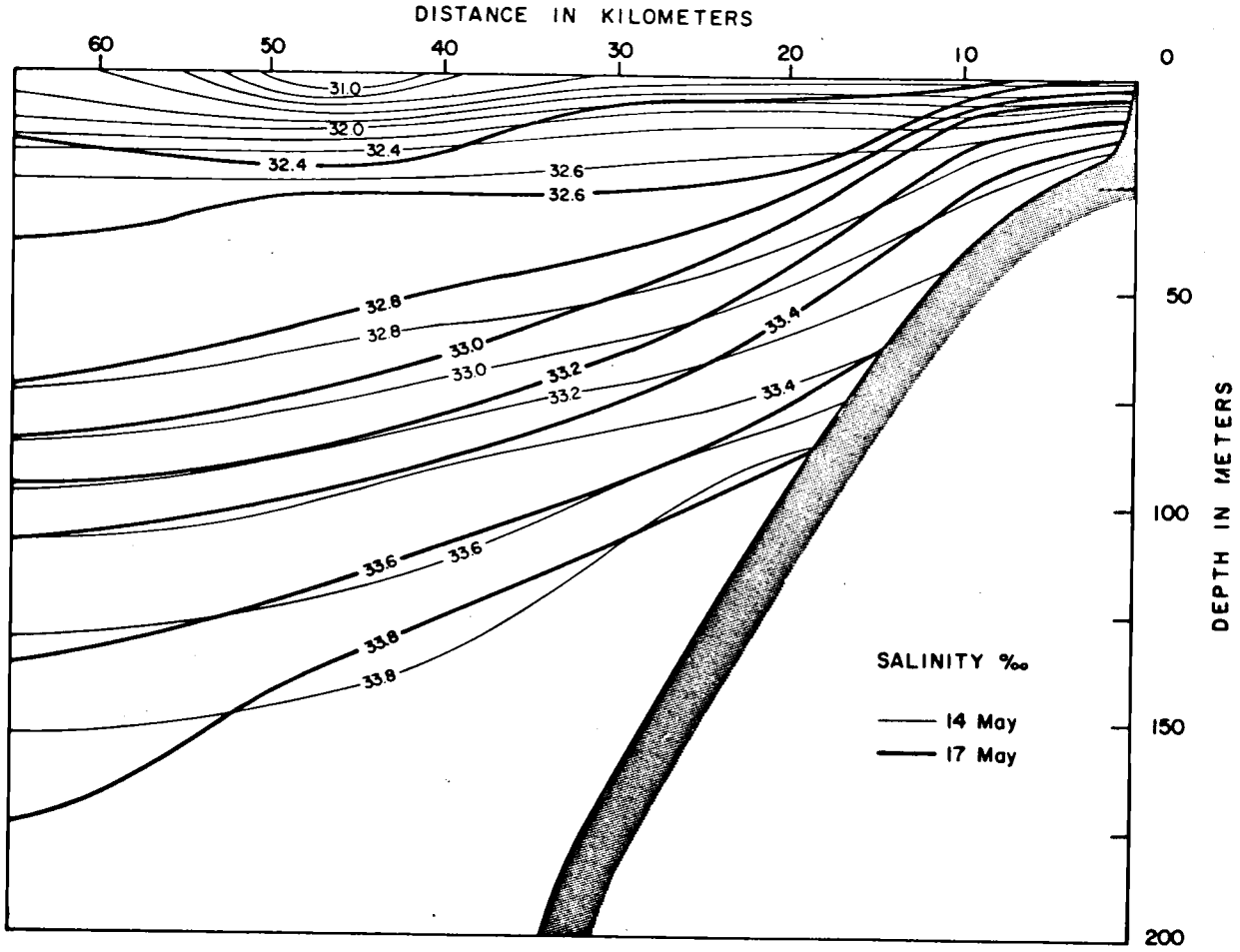

Figure 5. Salinity distribution along Brookings line in May 1963.

The total offshore transport through the station furthest from the shore (35 nautical miles) computed from salinity observations was 8.6×10^9 gr/cm and from temperature observations was 7.6×10^9 This flowed offshore between the surface and about 90 meters. The horizontal velocity is offshore above the 10° centigrade isotherm and the $33^{\circ}/oo$ isohaline. This corresponds to a sigma-t value of 25.4. The agreement is within computational error of identity with the value of 25.5, which has been assumed to indicate the bottom of the surface or drift current layer off Oregon in the model. The transport may also be found from the displacement of the 25.5 sigma-t surface between the two observations. This gives the amount of water transported offshore in the surface layer between sets of observations as 7.2×10^9 gr/cm.

The uncertainty in the values for the total transport is difficult to assess. An estimate of the uncertainty can be made from the observed standard deviation of the 25.5 sigma-t surface during a 24 hour series of observations at a station 23 nautical miles from the coast at $44^{\circ}39'$ north latitude. The standard deviation was about two meters. This includes the effect of any internal tidal oscillation which can seriously effect hydrographic data (4, vol. 2, p. 537-550). Since the stations on the Brookings line were occupied on the same phase of the tide, the uncertainty is less. An estimate of the

uncertainty in the total transport is of the order of 1×10^9 gr/cm.

These values of offshore transport, computed from the hydrographic observations, can be compared with the values from the model. The wind stress at 42° north latitude, 125° west longitude was computed from the 0000 and 1200 hours (Greenwich time) sea level pressure charts for 14 May through 17 May. The wind stress was computed from the geostrophic winds and the wind stress components averaged, yielding a resultant mean wind stress component for the y-direction of -1.60 dynes/cm^2. This implies an offshore transport of 4.4×10^9 gr/cm for the time between observations (27.4×10^4 sec). The wind stress was also computed from the shipboard observations of the wind. Since these observations were not spaced equally in distance or time, a selection of observations or a weighted mean was used to obtain a mean wind stress. Depending on the procedure or selection, one obtains values ranging from -1.56 to -3.80 dynes/cm^2 for τ_y, leading to a total offshore transport ranging from 4.4×10^9 to 8.8×10^9 gr/cm for the period.

The vertical velocity can be estimated from the change in depth of the 25.5 sigma-t surface between observations. The values obtained may be compared with those predicted by equation (49). The nominal coastline and the effective coastal boundary for the model should not be expected to coincide, due to the gradual slope of the sea

bottom in the immediate vicinity of the beach. The effective coastal boundary of 42° north latitude is taken arbitrarily at the 10-fathom line, or about two nautical miles from the coastline. Comparison of the values predicted by equation (49) taking $k = 0.70 \times 10^{-6}$ cm^{-1} and those observed from the displacement of the 25.5 sigma-t surfaces at 5, 15, 25 and 35 nautical miles from the coastline are given in Table 4. The estimated uncertainty in the observed vertical velocities is based on an estimated uncertainty of one meter in the depth of the sigma-t surface.

Table 4. Observed and predicted vertical velocities along 42° north latitude, 14 to 17 May 1964.

Distance from coastline	Observed vertical velocity 10^{-3} cm/sec	Predicted vertical velocity 10^{-3} cm/sec
5	7.0 ± 1.0	8.5
15	5.0 ± 1.0	2.1
25	2.3 ± 1.0	0.5
35	0.2 ± 1.0	0.1

The major part of the oceanographic data available have come from the regular hydrographic cruises operating on a monthly or bi-monthly schedule. The values of the parameters in the model are taken as monthly or longer term averages for this part of the discussion.

The amount of water upwelled and transported offshore per unit meridional length in a unit time can be computed using equation (49).

$$-M_x\Big|_{x=-L} = \int_{-L}^{0} \rho w_{-h}\, dx$$

The vertical velocity at the base of the surface or drift current layer, w_{-h}, can be estimated from the change in depth of the 25.5 sigma-t surface between cruises. This assumes no transport of mass across the sigma-t surface, an assumption that will be discussed below. The offshore limit, -L, is taken as the station 45 nautical miles off the coast.

In practice, the total transport between cruises was obtained by computing the volumetric changes in the surface layer due to the translation of the 25.5 sigma-t surface. The change in area between observations was found for the section in the xz-plane defined by the coastline, the vertical at 45 nautical miles off the coast, the sea surface and the 25.5 sigma-t level. Only the latter, of course, varied. These values for the total surface layer zonal transport are given in Table 5 for the upwelling season. Since the data from which these total transports were computed were obtained without regard to the tidal phase, the uncertainty is greater than that for the Brookings section discussed above. In addition, the sections extend further offshore. The uncertainty is estimated as 3×10^9 gr/cm.

Table 5. Zonal surface layer transport through meridional plane at 44° 39' north latitude, 125° 07' west longitude

Dates	Total transport from wind stress 10^9 gr/cm	Total transport from hydrographic data 10^9 gr/cm
1961		
23 Apr - 24 May	- 2.1	- 6.6
24 May - 27 June	- 2.0	- 8.0
27 June - 21 Aug	-15.6	-14.1
21 Aug - 30 Oct	- 8.2	+ 7.2
1962		
3 May - 6 June	-11.9	- 8.0
6 June - 27 July	-14.2	-22.5
27 July - 5 Sept	- 4.1	+ 2.3
1963		
25 May - 17 July	-12.2	- 9.5
17 July - 19 Sept	- 5.5	+ 1.2

According to the model the transport is a function of the mean meridional component of the wind stress. The average wind stress was computed for each month from the monthly mean pressure charts. The total zonal transport in the surface layer between sets of observations was found by weighting the monthly means according to the number of days in each month contained in the period. Some error may be introduced since the mean wind stress is computed from the entire month. This error is usually small since most observations were taken within a few days of the beginning of a month. More serious sources of uncertainties in the wind stress were discussed in Section IV and include the uncertainties in the wind stress formula itself, the relation between the geostrophic wind and the surface wind, and the averaging process itself. The uncertainty might be as large as a factor of two and the computed stresses are more likely to be underestimates. The total transports computed from the average wind stress are compared with those obtained from the oceanographic data in Table 5.

There have been few direct measurements of the currents off the Oregon coast during the upwelling season. The data for surface currents has been summarized by Maughan (18, p. 33). He found definite offshore flow in July and possibly weak offshore flow in June and August.

The agreement between the transport calculated from the north-south component of the wind stress and from the hydrographic data is very likely as good as can be expected. There are two basic sources of uncertainties in the values: the estimation of the mean wind stress and the assumption that the rate of change of the depth of the pycnocline layer is the vertical velocity of the water.

The assumption was made that the vertical velocity of the water at the base of the surface layer could be found by observing the change in depth of the 25.5 sigma-t surface with time. This assumes that there was no transfer of mass across the sigma-t surface. However, the possibility of mixing was explicitly allowed for in the model. While it is likely that, at least in the earlier portion of the upwelling season, the rate of ascent of the 25.5 sigma-t surface closely approximates the vertical velocity, this may not be so later in the upwelling season. Later in the upwelling season the slope of the pycnocline layer makes lateral mixing across the pycnocline a distinct possibility. Yoshida (52, p. 14-16) in his study asserts that an equilibrium is reached in which lateral mixing completely balances the vertical advection of density, resulting in a stationary pycnocline. Indeed, the pycnocline is observed to be stationary in the late summer or early fall off Oregon. It would appear from the position of the 25.5 sigma-t surface that there has been no offshore transport, or

even that there has been onshore transport, while the wind stress predicts continued upwelling and offshore transport.

The possibility that lateral mixing across the pycnocline could account for the stationary pycnocline in the presence of upwelling was tested. Assuming that the vertical advection of density and salt were balanced by lateral mixing, the eddy coefficient can be obtained from equation (37). For the stationary distribution of a property, S, the equation reduces to

$$w \frac{\partial S}{\partial z} = \frac{A_H}{\rho} \frac{\partial^2 S}{\partial x^2}$$

This equation was used with density and with salinity to find the lateral eddy diffusivity coefficient. The hydrographic data for October 1961, September 1962 and September 1963 were examined. The gradients of density and salinity were obtained using the values at 5, 15 and 25 nautical miles off the coast. The vertical velocity was assumed to be 10^{-3} cm/sec. The calculations were done for density and salinity independently and the extreme range of values for the transfer or mixing coefficient was from 0.5×10^6 to 3.4×10^6 c.g.s. units. These coefficients are in close agreement with values expected in this region (see Section II, The Theory of Hidaka).

In the fall the wind circulation pattern shifts with southerly winds becoming predominant. From October until May the monthly mean meridional wind stress is usually positive (Figure 2). Onshore

transport in the surface layer and subsidence of the pycnocline near the coast is therefore expected and does occur. However, the uncertainties in both the depth of the pycnocline and the mean wind stress are large. The pycnocline is frequently below the deepest sampling depth at the near shore stations (5 and 15 nautical miles from the coast) in the late fall and winter. The wind constancy parameter is very low with only 25% to 40% of the winds in the the same quadrant as the resultant wind during the fall and winter (42, p. 8-14), making the estimates of the mean wind stress less reliable. The indication is that from September or October to December or January an amount of water roughly equal to that transported offshore during the upwelling season is transported onshore. The subsidence of the 25.5 sigma-t surface from 30 October 1961 to 5 January 1962 indicates a total surface layer transport through the meridional section at 44°39' north latitude, 125°07'west longitude to be 19.6×10^9 gr/cm onshore. The meridional component of the mean wind stress predicts 9.6×10^9 gr/cm onshore transport for the period. For the period from 5 September 1962 to 17 December 1962 the subsidence of the 25.5 sigma-t surface and the mean meridional wind stress yield values of 35.4 gr/cm and 30.2 gr/cm, respectively, for the onshore transport during the period. The transports are variable during the late winter and early

spring and the net transport from January until the beginning of upwelling appears minor. In the late spring the atmospheric circulation again shifts and northerly winds predominate, and upwelling commences.

VI. SUMMARY AND CONCLUSIONS

Upwelling is one of the more significant oceanographic phenomena of the Oregon oceanic waters. Its effects range from keeping the water too cool for comfortable swimming in the summer to increasing the productivity of the coastal waters.

In general, upwelling is the result of the horizontal divergence of the surface layer, resulting in subsurface water rising into the surface layer. The divergence may be induced by a longshore wind stress in the coastal region, or by the spatial variation of the wind stress in the open ocean. Coastal upwelling is an order of magnitude more intense than open ocean upwelling but is limited to within about 100 kilometers of the coast.

Coastal upwelling along the Oregon coast is clearly associated with a northerly wind stress. Along the Oregon coast the winds are favorable for upwelling from about May to September, the months during which the oceanographic data show upwelling.

The idealized model of this study encompasses both open ocean and coastal upwelling. The model gives the vertical velocity at the base of the surface layer, which is represented by the 25.5 sigma-t surface off the Oregon coast. The model cannot quantitatively predict the effect of upwelling on the distribution of properties in the surface

layer. The three-layer nature of the model, while a fair approximation to the density structure and therefore useful in the dynamical study, is too idealized for a quantitative description of the distribution of other properties. The distribution of properties within the surface layer is critically dependent on both horizontal and vertical mixing, which are yet imperfectly understood in the ocean. The model itself would fail if the pycnocline were close enough to the surface so that horizontal and vertical mixing would eliminate the density stratification. This has been observed to occur off Oregon, though only very near shore.

Should more oceanographic and meteorological data become available, from such sources as offshore moored buoys, it would perhaps be worthwhile to retain the wind stress variations in equation (42) and to allow the parameter, k, to vary. The model as it stands does, however, provide qualitative agreement with observations and in the case of coastal upwelling some degree of quantitative agreement. Oceanographic data have been used to infer vertical velocities at the base of the surface layer and the amount of water upwelled in the coastal region. These values have been compared with the values predicted from the meridional component of the wind stress on the basis of the model. The quantitative agreement may be as good as can be expected since the ocean is a difficult laboratory. The

venerable oceanographer Defant, however, deserves the final word:

> A totally satisfying explanation of upwelling at continental coasts has not yet been given, and is probably not possible at all since the total process is composed of a number of substages each of which is always controlled by other factors (4, vol. 1, p. 652).

BIBLIOGRAPHY

1. Bowden, K. F. Turbulence. In: The sea. vol. 1. New York, Interscience, 1962. p. 802-825.

2. Collins, Curtis A. Structure and kinematics of the permanent oceanic front off the Oregon coast. Master's thesis. Corvallis, Oregon State University, 1964. 53 numb. leaves.

3. Currie, Ronald. Upwelling in the Benguela Current. Nature 171:497-500. 1953.

4. Defant, Albert. Physical oceanography. New York, Pergamon, 1961. 2 vols.

5. Ekman, V. Walfrid. On the influence of the earth's rotation on ocean currents. Arkiv for Matematik, Astronomi och Fysik 2 (11):1-52. 1905.

6. Eliassen, A. and E. Kleinschmidt, Jr. Dynamic meterorology. In: Handbuch der Physik. Bd. 48. Berlin, Springer-Verlag, 1957. p. 1-154.

7. Fofonoff, N. P. Machine computation of mass transport in the North Pacific Ocean. Journal of the Fisheries Research Board of Canada 19:1121-1141. 1962.

8. Fofonoff, N. P. and F. W. Dobson. Transport computations for the North Pacific Ocean 1950-1959. Nanaimo, 1963. 179 numb. leaves. (Fisheries Research Board of Canada. MS. Report Series No. 166)

9. Freeman, John C. Note on a prediction equation for the surface layer of a two-layer ocean. Transactions of American Geophysical Union 35:585-587. 1954.

10. Green, C. K. Summer upwelling - northeast coast of Florida. Science 100:546-547. 1944.

11. Gunther, E. R. A report on oceanographical investigations in the Peru Coastal Current. Discovery Reports 13:107-276. 1936.

12. Hachey, H. B. Ekman's theory applied to water replacements on the Scotian shelf. Proceedings of the Nova Scotian Institute of Science 19:264-276. 1937.

13. Hart, T. John and Ronald I. Currie. The Benguela Current. Discovery Reports 31:123-298. 1960.

14. Hidaka, Koji. A contribution to the theory of upwelling and coastal currents. Transactions of the American Geophysical Union 35:431-444. 1954.

15. Hidaka, Koji. Computations of the wind stress over the oceans. Records of Oceanographic Works in Japan, new ser., 4 (2): 77-123. 1958.

16. Longard, J. R. and R. E. Banks. Wind induced vertical movement of the water on an open coast. Transactions of the American Geophysical Union 33:377-380. 1952.

17. Malkus, Joanne S. Interchange of properties between sea and air: Large-scale interactions. In: The sea. vol. 1. New York, Interscience, 1962. p. 88-294.

18. Maughan, Paul M. Observation and analysis of ocean currents above 250 meters off the Oregon coast. Master's thesis. Corvallis, Oregon State University, 1963. 49 numb. leaves.

19. McEwen, George F. The distribution of oceanic temperatures along the west coast of North America deduced from Ekman's theory of the upwelling of cold water from the adjacent ocean depths. Internationale Revue der gesamten Hydrobiologie und Hydrographie 5:243-286. 1912.

20. McEwen, George F. Rate of upwelling in the region of San Diego computed from serial temperatures. In: Proceedings of the Fifth Pacific Science Congress, Victoria, 1933. vol. 3. Toronto, University of Toronto Press, 1934. p. 1763.

21. McEwen, George F. The dynamics of large horizontal eddies (axes vertical) in the ocean off southern California. Journal of Marine Research 7:188-216. 1948.

22. Moffett, James W. An instance of upwelling along the east shore of Lake Michigan, 1955. In: Proceedings of the Fifth Conference on Great Lakes Research, Toronto, 1962. Ann Arbor, University of Michigan Press, 1962. p. 126.

23. Montgomery, R. B. Transport of surface water due to the wind system over the North Atlantic. Papers in Physical Oceanography and Meterorology 4 (3):23-30. 1936.

24. Munk, Walter H. A critical wind speed for air-sea boundary processes. Journal of Marine Research 6:203-218. 1947.

25. Park, Kihlo, June G. Pattullo and Bruce Wyatt. Chemical properties as indicators of upwelling along the Oregon coast. Limnology and Oceanography 7:435-437. 1962.

26. Pattullo, June G. Upwelling, fact and fancy. Paper read before the 13th annual meeting of the Pacific Northwest Oceanographers, Seattle, February 8, 1964.

27. Pearson, Erman A. and George A. Holt. Water quality and upwelling at Grays Harbor entrance. Limnology and Oceanography 5:48-56. 1960.

28. Posner, Gerald S. The Peru Current. Bulletin of the Bingham Oceanographic Collection 16:106-155. 1957.

29. Proudman, J. Dynamical oceanography. London, Methuen, 1953. 409 p.

30. Reid, Joseph L., Jr., Gunner I. Roden and John G. Wylie. Studies of the California Current system. California Cooperative Oceanic Fisheries Investigations Progress Reports, January 1, 1958, p. 27-57.

31. Richards, Francis A. Some chemical and hydrographic observations along the north coast of South America - I. Deep-Sea Research 7:163-182. 1960.

32. Rossby, C.-G. On the frictional force between air and water and on the occurrence of a laminar boundary layer next to the surface of the sea. Papers in Physical Oceanography and Meterorology 4 (3):3-20. 1936.

33. Rossby, C.-G. and R. B. Montgomery. The layer of frictional influence in wind and ocean currents. Papers in Physical Oceanography and Meterorology 3 (3):1-101. 1935.

34. Scripps Institution of Oceanography. The field of mean wind stress over the North Pacific Ocean. La Jolla, 1948. 70 p. (Oceanographic Report No. 14)

35. Stommel, Henry. On the determination of the depth of no meridional motion. Deep-Sea Research 3:273-278. 1956.

36. Sverdrup, H. U. Oceanography. In: Handbuch der Physik. Bd. 48. Berlin, Springer-Verlag, 1957. p. 608-670.

37. Sverdrup, H. U. On the process of upwelling. Journal of Marine Research 1:155-164. 1938.

38. Sverdrup, H. U. and R. H. Fleming. The waters off the coast of southern California March to July, 1937. Bulletin of the Scripps Institution of Oceanography 4:261-378. 1941.

39. Sverdrup, H. U., Martin W. Johnson and Richard H. Fleming. The oceans, their physics, chemistry and general biology. New York, Prentice-Hall, 1942. 1087 p.

40. Taylor, C. B. and H. B. Stewart, Jr. Summer upwelling along the east coast of Florida. Journal of Geophysical Research 64:33-40. 1959.

41. Taylor, G. I. Skin friction of the wind on the earth's surface. Proceedings of the Royal Society, ser. A, 92:196-199. 1916.

42. U.S. Weather Bureau. Atlas of climatic charts of the oceans. 1938. 65 p. (Weather Bureau No. 1247)

43. Welander, Pierre. Wind action on a shallow sea: Some generalizations of Ekman's theory. Tellus 9:45-52. 1957.

44. Wells, Harry W. and I. E. Gray. Summer upwelling off the northeast coast of North Carolina. Limnology and Oceanography 5:108-109. 1960.

45. Wilson, Basil W. Note on surface wind stress over water at low and high wind speeds. Journal of Geophysical Research 65:3377-3382. 1960.

46. Wooster, Warren S. El Nino. California Cooperative Oceanic Fisheries Investigations Reports 8:43-45. 1960.

47. Wooster, Warren S. and Joseph L. Reid, Jr. Eastern boundary currents. In: The sea. vol. 2. New York, Interscience, 1963. p. 253-280.

48. Wooster, Warren S. and Bruce A. Taft. On the reliability of field measurements of temperature and salinity in the ocean. Journal of Marine Research 17:552-566. 1958.

49. Wyatt, Bruce and N. F. Kujala. Hydrographic data from Oregon coastal waters June 1960 through May 1961. Corvallis, 1962. 77 numb. leaves. (Oregon State University, Department of Oceanography, Ref. 62-2, Data Report No. 7)

50. Wyrtki, Klaus. The upwelling in the region between Java and Australia during the south-east monsoon. Australian Journal of Marine and Freshwater Research 13:217-225. 1962.

51. Wyrtki, Klaus. The horizontal and vertical field of motion in the Peru Current. Bulletin of the Scripps Institution of Oceanography 8:313-346. 1963.

52. Yoshida, Kozo. Coastal upwelling off the California coast. Records of Oceanographic Works in Japan, new ser., 2(2):8-20 1955.

53. Yoshida, Kozo. Coastal upwelling off the California coast and its effects on productivity of the waters. In: Proceedings of the UNESCO Symposium on Physical Oceanography, Tokyo, 1955. Paris, UNESCO, 1957. p. 104-106.

54. Yoshida, Kozo. An example of variations in oceanic circulation in response to variations in wind field. Journal of the Oceanographic Society of Japan 11:103-108. 1955.

55. Yoshida, Kozo. A note on the pressure change of the two-layer ocean. Journal of the Oceanographic Society of Japan 12:111-116. 1956.

56. Yoshida, Kozo. A study of upwelling. Records of Oceanographic Works in Japan, new ser., 4(4):186-192. 1958.

57. Yoshida, Kozo and Han-Lee Mao. A theory of upwelling of large horizontal extent. Journal of Marine Research 16:40-53. 1957.

APPENDIX

LIST OF SYMBOLS

b ..... bottom

f ..... Coriolis parameter = $2\omega \sin\varphi$

g ..... acceleration of gravity

h ..... depth of surface layer

k ..... $f/\sqrt{(\Delta\rho/\rho)\, gh}$

p ..... pressure

u, v, w ..... velocity components in the x, y, z directions

$\vec{u}_a$ ..... wind velocity

w_{-h} ..... vertical velocity at base of surface layer

x ..... horizontal coordinate, directed eastward

y ..... horizontal coordinate, directed northward

z ..... vertical coordinate, directed upward

A_H ..... horizontal coefficient of eddy viscosity

A_V ..... vertical coefficient of eddy viscosity

C_D ..... drag coefficient of wind on sea surface

D_H ..... horizontal frictional distance

D_V ..... depth of frictional influence

L ..... width of coastal upwelling region

M_x ..... zonal mass transport

M_y ..... meridional mass transport

S ..... concentration of a conservative property

β ..... meridional gradient of Coriolis parameter

ζ .... vertical component of relative vorticity

ξ .... elevation of sea surface

ρ .... density of water

ρ_1, ρ_2 .... density of surface and deep layer

$\Delta\rho$ .... difference in density between deep and surface layers

ρ_a .... density of air

σ_t .... sigma-t = $10^3(\rho - 1)$, measured at atmospheric pressure

τ_x, τ_y .... components of the wind stress on the sea surface

τ_{xz}, τ_{yz} .... components of shearing stress across a horizontal surface

φ .... latitude

ω .... earth's angular velocity